Received: 26 October 2021 | Revised: 22 January 2022 | Accepted: 30 January 2022

IET Generation, Transmission & Distribution

DOI: 10.1049/gtd2.12423

The Institution of Engineering and Technology WILEY

ORIGINAL RESEARCH PAPER

A tactical scheduling framework for wind farm-integrated multi-energy systems to take part in natural gas and wholesale electricity markets as a price setter

Nima Nasiri[1] | **Saeed Zeynali**[1] | **Sajad Najafi Ravadanegh**[1] | **Mousa Marzband**[2]

[1] Resilient Smart Grids Research Lab, Electrical Engineering Department, Azarbaijan Shahid Madani University, Tabriz, Iran

[2] Northumbria University, Electrical Power and Control Systems Research Group, Newcastle upon Tyne, UK

Correspondence
Sajad Najafi Ravadanegh, Resilient Smart Grids Research Lab, Electrical Engineering Department, Azarbaijan Shahid Madani University, Tabriz, Iran.
Email: s.najafi@azaruniv.ac.ir

Abstract

The wind integrated multi-energy systems (MES) have gained significant momentum in recent years on account of their self-sufficiency and attractive clean attributes. This study puts forward a bi-level multi-follower optimization framework to study the tactical response of a wind integrated MES in the wholesale electricity market (WEM) and the natural gas market (NGM) as a price setter. At the upper level, the MES endeavors to minimize the overall operational costs by giving the best offer/bid in WEM/NGM, and by utilizing thermal energy storage (TES), compressed air energy storage (CAES), and natural gas storage (NGS). When the MES submits offers/bids in WEM and NGM, the NGM and WEM operators, as individual followers, clear their respective markets to maximize public welfare and announce the ultimate market-clearing price (MCP). Additionally, risk-averse and risk-seeker information gap decision theory (IGDT) have been deployed to provide various decision-making options for MES operators considering wind underproduction and overproduction scenarios. Standard 6-node natural gas network (NGN) and 6-bus transmission system (TS) have been deployed to model WEM and NGM, respectively. The results testify to the capabilities of the MES in influencing the decisions of WEM and NGM.

1 | INTRODUCTION

1.1 | Background and motivation

In competitive markets, some participants might be considered as strategic entities, which can influence market outcomes with their decisions [1]. In recent years, various strategic players have been studied in different energy market levels, including the thermal units in wholesale electricity markets (WEM) [2], virtual power plants in the day-ahead wholesale market [3], and the distribution company in WEM [4]. The purpose of these models is to reach a state of equilibrium between strategic participants and the electricity market. These models do not only outline the optimal strategy for the market participants but also aid the system operator to keep the market under surveillance and enact regulatory policies accordingly [5]. That said, the majority of these studies have only examined a single type of energy, that is, electricity. In contrast, co-generation units, such as combined heat and power (CHP) units, electrical boilers (EB), and thermal pumps, have diverted the attention of researchers to other energy varieties (e.g., natural gas, and local thermal energy) [6]. Consequently, multiple aspects of multi-energy systems have been under comprehensive scrutiny. This MES can appear in the form of commercial, industrial, and agricultural sites , or they can represent a portion of a city [7] that are integrated with renewable generation units such wind turbines (WT). To procure their demand, the MES can simultaneously participate in WEM and natural gas market (NGM). Considering the rising penetration of MESs in various energy markets, their behavior can impose a substantial influence on the market outcomes [8]. To this end, the tactical (or strategic) behavior of an MES in transactions with WEM and NGM as a price influencer is scrutinized. In this regard, a bi-level multi-follower framework is proposed, where the NGN and WEM are independent followers for MES that is the leader. Using the Karush-Kuhn-Tucker (KKT) conditions, the problem is reformulated a single-level

mathematical problem with equilibrium constraints (MPEC), which ensures equilibrium between markets and MES.

1.2 | Literature review

There have been various studies on different facets of MES including different management strategies [9], reliability assessments [10], environmental emission reduction [11], flexibility improvements [12], and resilience [13]. Another novel subject that has recently been in the center of attention is the way in which MES takes part in different levels of the market; particularly, in transactions with WEM, NGM and other competitive rivals. In [14], a risk-based framework was proposed for MES to participate in WEM considering compressed air energy storage (CAES), thermal energy storage (TES) and natural gas storage (NGS). Moreover, a chance-constrained two-stage stochastic programming approach was investigated in [15] for MES to join in day-ahead and real-time markets. Similarly, a stochastic decision-making framework was investigated in [16] for MES to participate in reserve and day-ahead markets. The authors in [17] scrutinized a hybridized stochastic programming (SP) and robust optimization (RO) model for an electricity retailer to seize the arbitrage opportunities. An analogous hybrid framework was also proposed in [18] to model MES behavior in NGM, day-ahead, real-time and local markets. Khorasany et al. [19] inspected a transactive energy framework for optimal energy management of multiple MESs, wherein at the first stage, the MES trades its surplus/deficit energy in the local electricity market, while at the second stage, MESs get involved in trades with various energy markets. Furthermore, a self-scheduling framework was proposed in [20] for an MES to participate in thermal and electrical markets and maximize its profit under information gap decision theory (IGDT).

The strategic behavior of energy players in different markets is another hot research topic. In energy markets, a strategic player is a participant that can have influence on the market price by its decisions. Therefore, there has been many bi-level or multi-level studies on the tactical market response of MESs. To evaluate the trade ties of MES in local electricity distribution markets, the authors in [21] suggested a bi-level framework, where the distribution system and MES were modeled at upper and lower levels, respectively. Additionally, profit-oriented tactical scheduling of an MES in local electricity and thermal energy markets have been studied in [22]. The model includes MES profit maximization at upper level, while the lower level embodies the market clearing procedure to maximize public satisfaction. The authors in [23] have scrutinized the tactical behavior of MES players in transactions with WEM and local energy systems. Maximization of social welfare and profit of local energy system was integrated ay second level, while profit maximization of MESs made the upper level. A two-stage SP model was proposed in [24] to study the optimal MES response in trades with pool market, NGM and forward contracts considering the existence of other completive market participants. The study incorporates competitive rivals of MES at the lower level, while MES is considered to be the leader. A two-step iteration-based framework has been studied in [25] to evaluate the tactical stochastic response of an MES in integrated natural gas and electricity markets. The first step consists of optimal dispatching of units in MES, and at the second step, the NGM and WEM are scheduled in accordance to the MES decisions. Moreover, a bi-level framework has been studied in [26] to model the trades between retail multi-energy markets and multi-energy consumers, where retail markets and multi-energy consumers form the upper and lower levels A bi-level optimization framework with single follower was developed by [27], where the leader problem is the profit maximization of integrated power and gas energy provider. The study integrated the WEM as the lower level follower

Because of their high storage capacity and low capital investment requirements, the CAES units have been the cornerstone of ancillary service markets [28]. In this respect, a hybrid SP-RO method has been proposed by [29] to evaluate the role of CAES in day-ahead and real-time markets. Likewise, an SP-RO tactical bidding/offering framework for CAES units has been studied in [30] to maximize profit. The intermittent nature of wind power is addressed by a CAES in [31], which is also subjected to unit commitment and power system constraints. The study proposes the IGDT approach to deal with unknown parameter values. To manage the high penetration of wind energy, ref [32] proposes a CVaR-constrained CAES and TES operation scheduling framework.

1.3 | Contributions

The main differences between this work and other studies can be observed in Table 1. The chief downsides (DS) of the publications mentioned above are listed as follows:

- **DS1**: In studies [9–21, 23, 24, 26, 28, 29, 31], the MES partakes in various markets as a price taker. Nevertheless, a price taker does not have any authority over market clearing price (MCP), and it is obliged to conform to the market price announced by the market operator.
- **DS2**: The studies [9–20, 23, 24, 26, 28, 29, 31] have investigated the behavior and partition means of MES in different market levels. That said, the operational mechanism and behavior models of the markets have been neglected. Modelling the limitations and mechanism of the natural gas network (NGN) and transmission system (TS) is vitally important in calculation of MCP. Disregarding their models renders these studies incompatible with practical circumstances.
- **DS3**: Some of these studies (i.e., [9–13, 15, 16, 19, 21–27]) have not evaluated the CAES's presence in the tactical scheduling of MES as a price setter in various energy markets. A CAES can be operated together with a TES and NGS to enhance the role of MES in markets and manage the uncertainties derived from volatile wind power.
- **DS4**: The studies [9–18, 21–29 31] have proposed RO and SP methods. However, the SP method requires complicated

TABLE 1 Comparative evaluations between this study and previous publications

	Strategic behavior		Network constraints				
Ref	**Price taker**	**Price maker**	**Gas**	**Electricity**	**CAES**	**Bi-level model**	**Uncertainty modeling**
[9]	√	×	×	×	×	×	-
[10]	√	×	×	×	×	×	-
[11]	√	×	×	×	×	×	Stochastic
[12]	√	×	×	×	×	×	-
[13]	√	×	×	×	×	×	Robust
[14]	√	×	×	×	√	×	Stochastic
[15]	√	×	×	×	×	×	Stochastic
[16]	√	×	×	×	×	×	Stochastic
[17]	√	×	×	×	√	×	Robust-stochastic
[18]	√	×	×	×	√	×	Robust-stochastic
[19]	√	×	×	×	×	×	Stochastic
[20]	√	×	×	×	√	×	IGDT
[21]	√	×	×	√	×	√	-
[22]	×	√	×	√	×	√	-
[23]	√	×	×	×	×	√	Stochastic
[24]	√	×	×	×	×	√	Stochastic
[25]	×	√	√	√	×	√	Stochastic
[26]	√	×	×	×	×	×	-
[27]	×	√	√	√	×	√	Robust
[28]	√	×	×	×	√	×	Robust-stochastic
[29]	√	×	×	×	√	×	Stochastic
[30]	×	√	×	×	√	×	Robust-stochastic
[31]	√	×	×	×	√	×	IGDT
[32]	√	×	×	×	√	×	Stochastic
This study	×	✓	✓	✓	✓	✓	**IGDT**

risk measures, and RO can only provide risk averse solutions, while in real-world applications, the MES operator should have a choice between risk-averse or risk seeker frameworks. Moreover, the MES operator might want to define the amount of cost that it is willing to pay for the risk, which is not possible in RO and SP methods. The SP method requires the existence of probability distribution functions, which are unavailable for most of the real-world parameters.

To cover these DSs, this paper proposes a bi-level single-leader multi-follower framework to evaluate the tactical behavior of a wind farm-integrated MES in transactions with WEM and NGM as a price setter considering multi-carrier energy storages (MCES). At the primary level, the MES operator seeks the minimization of overall operational costs by submitting the best offer/bid in WEM/NGM, as well as deploying MCESs, such as TES, NGS and CAES. At the secondary level, the WEM/NGM operators, as individual follower operators, clear the market aiming to maximize public welfare, considering the operational constraints of the NGN and TS. Utilizing the KKT conditions, and the theory of strong duality, the problem is redefined as a conventional single-level optimization problem that is solved by a standard mixed-integer linear programming (MILP) solver. Moreover, a risk-averse and risk-seeker IGDT approach is integrated with the problem to handle uncertain wind power production without the need for any probability distribution functions. Overall, the authentic novelties of this work are listed as follows:

1. A bi-level programming framework is proposed to scrutinize the tactical behavior of a wind integrated MES operator as a price setter in NGM and WEMs. (Eliminates **DS1**).
2. The impact of merging MCESs, such as TES, NGS and CAES on a price setter MES in NGM/WEM is evaluated considering TS and NGN constraints. (Addresses **DS2** and **DS3**).
3. The IGDT framework is adopted under two strategies, namely risk-seeker and risk-averse, to manage wind power uncertainties and evaluates its impact on MCP of NGM and WEM. (Accounts for **DS4**).

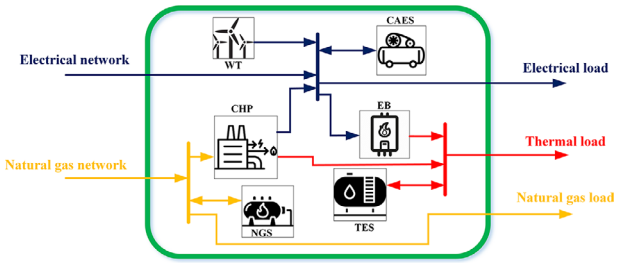

FIGURE 1 The structure of the suggested MES

2 | PROBLEM DESCRIPTION

The structural topology of the proposed MES is depicted in Figure 1. Accordingly, MES is equipped with a CHP unit, WT, EB, TES, CAES and NGS. Figure 2 illustrates the algorithmic flowchart of the decision-making process for the proposed MES in NGM and WEM as a price maker. In this algorithm, after obtaining the data and information, the MES operator (as a leader) submits offers/bids in NGM and WEM. At this point, the NGM and WEM receive the offers/bids from the MES operator and other market players, for example, generation companies (Genco) and gas wells. Afterwards, they clear their independent markets with the goal of achieving maximum social welfare. The market-clearing process yields lower-level decision variables, such as Genco production, gas well dispatch, power exchange of MES with NGM/WEM and MCP of NGM and WEM. The market-clearing alters the market dynamics, and the MES, therefore, reschedules itself to acclimatize to this new market environment. Then the MES resubmits bids/offers in WEM and NGM to purchase/sell energy. This repetitive interactive cycle between lower-level followers and the MES is conducted until reaching a state of market equilibrium. In this study, this algorithm was implemented by KKT conditions and the theory of strong duality, which convert the bi-level nonlinear problem into a single-level MILP. In such a mathematical model, the decisions of MES will prompt reactive response in WEM/NGM and vice versa, which is the reason that makes this model a price setter framework that is superior to non-interactive price-taker models.

3 | FORMULATION

The bi-level problem formulation for the upper and lower levels is established in this section. This problem is converted into a single-level model by KKT conditions and the theory of strong duality as depicted in [27].

3.1 | Multi-energy system model (leader)

3.1.1 | Objective function

Equation (1) defines the optimization objective function for the upper level. The function is composed of 7 terms. The first and the second term refer to the cost of purchasing electricity/gas from WEM/NGM. The operational costs in charge, discharge and simple cycle operation modes of the CAES are established by third to fifth terms. Eventually, the cost of utilizing NGS and TES is expressed by sixth and seventh terms.

$$OF = \min \sum_{h} \sum_{t} \left\{ \begin{array}{l} \lambda_{h,t} P_{h,t}^{MES} + \gamma_{n,t} G_{h,t}^{MES} \\ +C_{h,t}^{ch} P_{h,t}^{ch} + C_{h,t}^{dis} P_{h,t}^{dis} \\ +C_{h,t}^{si} P_{h,t}^{si} + C_{h,t}^{out} GS_{h,t}^{out} \\ +C_{h,t}^{Hch} H_{h,t}^{Hch} \end{array} \right\}. \quad (1)$$

3.1.2 | Combined heat and power unit (CHP)

Equations (2) and (3) consecutively circumscribe the electrical and thermal output of the CHP unit within the bounds of feasible operation region (FOR). The commitment status of CHP unit is established by Equation (4), while the linear coefficient variable of FOR is restricted by Equation (5). The natural gas consumption of the CHP unit is modelled by Equation (6). The FOR, which defines the interrelation between the thermal and electrical output of the CHP unit, is illustrated in Figure 3.

$$P_{h,t}^{CHP} = \sum_{R=1} \alpha_t^R P^R \quad \forall h, \forall t, \quad (2)$$

$$H_{h,t}^{CHP} = \sum_{R=1} \alpha_t^R H^R \quad \forall h, \forall t, \quad (3)$$

$$\sum_{R=1} \alpha_t^R = I_{h,t} \quad \forall h, \forall t, \quad (4)$$

$$0 \le \alpha_{t,R} \le 1, \quad \forall R, \forall t, \quad (5)$$

$$Q_{h,t}^{CHP} = \gamma_p P_{h,t}^{CHP} + \gamma_H H_{h,t}^{CHP} \quad \forall h, \forall t. \quad (6)$$

Equations (7) and (8), respectively, define the ramp up and ramp down limits of the CHP. Moreover, Equation (9) imposes the on/off status of the CHP. Evidently, the CHP cannot be on and off at the same time, which is ensured via Equation (10).

$$P_{h,t}^{CHP} - P_{h,t-1}^{CHP} \le \left[1 - Y_{h,t}\right] R_h^{up} + Y_{h,t} P_h^{\min} \quad \forall h, \forall t, \quad (7)$$

$$P_{h,t-1}^{CHP} - P_{h,t}^{CHP} \le \left[1 - Z_{h,t}\right] R_h^{dn} + Z_{h,t} P_h^{\min} \quad \forall h, \forall t, \quad (8)$$

$$Y_{h,t} - Z_{h,t} = I_{h,t-1} - I_{h,t} \quad \forall h, \forall t, \quad (9)$$

$$Y_{h,t} + Z_{h,t} \le 1 \quad \forall h, \forall t. \quad (10)$$

The minimum on time constraints of CHP is imposed by Equations (11)–(14). Likewise, Equations (15)–(18) enforce the

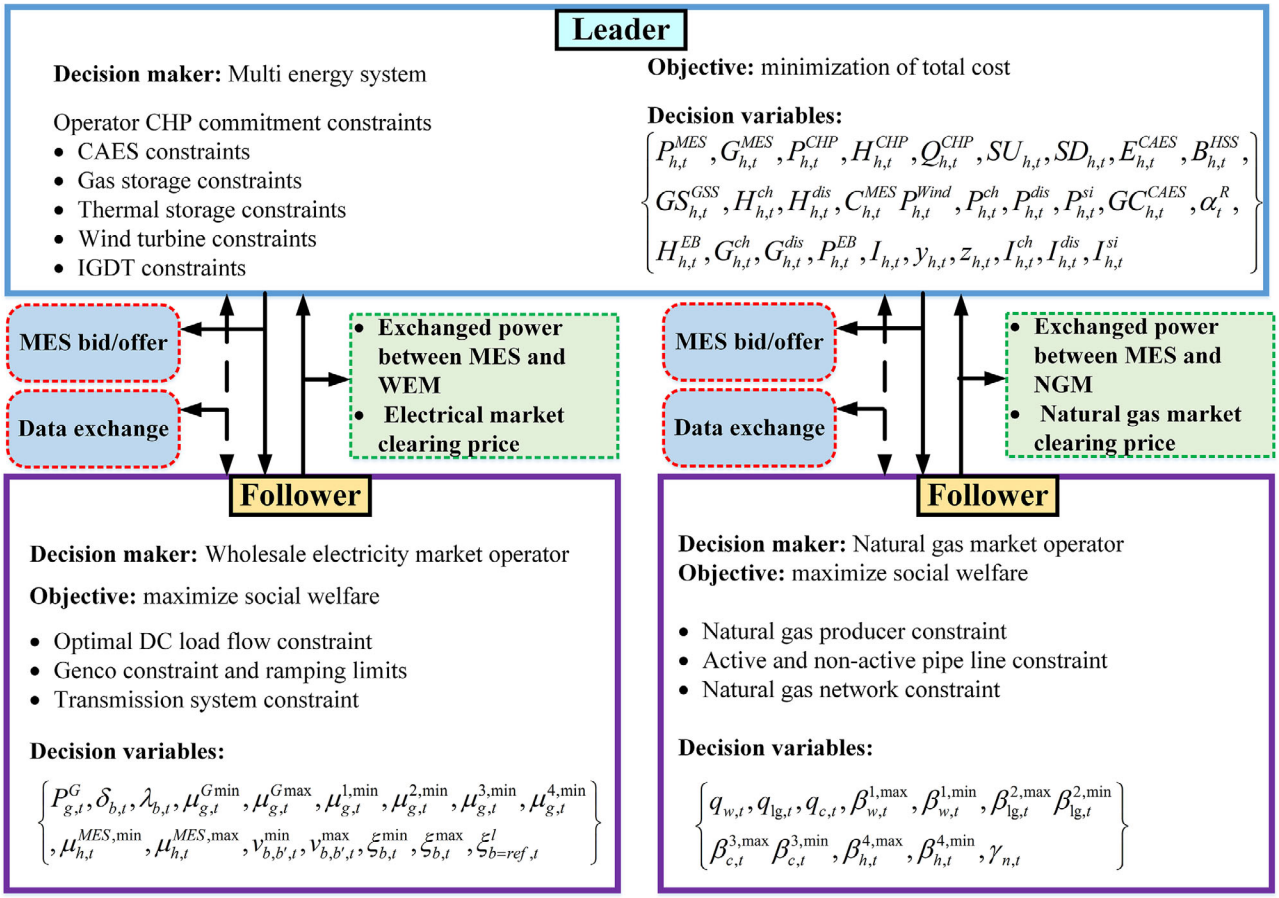

FIGURE 2 The algorithmic flowchart of the interaction between MES and WEM/NGM

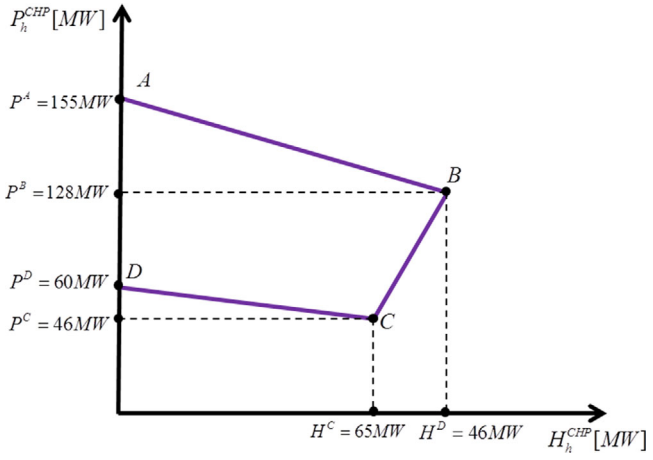

FIGURE 3 Feasible operation region (FOR) of CHP

minimum off time limits of CHP.

$$T_h^{Ue} = \min\left\{T, (T^U - T_h^{U0})I_{h,t=0}\right\}, \tag{11}$$

$$\sum_{t=1}^{T_h^{Ue}} I_{h,t} = T_h^{Ue} \ \forall h, \tag{12}$$

$$\sum_{t=r}^{t+T_h^{Ue}-1} I_{h,r} \geq T_h^U y_{h,t} \tag{13}$$

$$\forall h, \forall t = \left[T_h^{Ue} + 1, \ldots, T - T_h^U + 1\right],$$

$$\sum_{t=r}^{T} (I_{h,r} - y_{h,t}) \geq 0 \ \ \forall h, \forall t = \left[T - T_h^U + 2, \ldots .., T\right], \tag{14}$$

$$T_i^{De} = \min\left\{T, (T^D - T_h^{D0})(1 - I_{h,t=0})\right\}, \tag{15}$$

$$\sum_{t=1}^{T_h^{De}} I_{h,t} = 0 \ \ \forall h, \tag{16}$$

$$\sum_{t=r}^{t+T_h^D-1} (1 - I_{h,r}) \geq T_h^D z_{h,t} \tag{17}$$

$$\forall h, \forall t = \left[T_h^{De} + 1, \ldots .., T - T_h^D + 1\right],$$

$$\sum_{t=r}^{T} (1 - I_{h,r} - z_{h,t}) \geq 0 \ \ \forall h, \forall t = \left[T - T_h^D + 2, \ldots .., T\right]. \tag{18}$$

The amount of required fuel to turn the CHP on or off is defined by Equations (19) and (20), respectively.

$$SU_{h,t} \geq C_h^{SU} Y_{h,t} \quad \forall h, \forall t, \tag{19}$$

$$SD_{h,t} \geq C_h^{SD} Z_{h,t} \quad \forall h, \forall t. \tag{20}$$

3.1.3 | Compressed air energy storage (CAES)

The compressed air energy is stored in and released from CAES according to Equation (21). The storage state of CAES is bounded by Equation (22), while Equation (23) enforces the initial and final state of storage. The charge, discharge and simple cycle operation modes of CAES is established through Equations (24)–(26). Furthermore, the air cannot be compressed in and decompressed from CAES simultaneously, which is defined by Equation (27). Eventually, the natural gas demand of CAES during discharge and simple cycle operational states is calculated by Equation (28). In simple cycle mode, the storage is empty and the CAES consumes natural gas as a gas turbine to produce electrical energy. It is noteworthy that this mode is the most unproductive operational state since the efficiency is half of the discharge mode [14].

$$E_{h,t}^{CAES} = E_{h,t-1}^{CAES} + \eta_h^{ch} P_{h,t}^{ch} - \frac{P_{h,t}^{dis}}{\eta_h^{dis}} \quad \forall h, \forall t, \tag{21}$$

$$E_{h,t}^{\min} \leq E_{h,t}^{CAES} \leq E_{h,t}^{\max} \quad \forall h, \forall t, \tag{22}$$

$$E_{h,t=24}^{\min} = E_{h,t=1}^{\min} \quad \forall h, \forall t, \tag{23}$$

$$P_h^{ch,\min} I_{h,t}^{ch} \leq P_{h,t}^{ch} \leq P_h^{ch,\max} I_{h,t}^{ch} \quad \forall h, \forall t, \tag{24}$$

$$P_h^{dis,\min} I_{h,t}^{dis} \leq P_{h,t}^{dis} \leq P_h^{ch,\max} I_{h,t}^{dis} \quad \forall h, \forall t, \tag{25}$$

$$P_h^{si,\min} I_{h,t}^{si} \leq P_{h,t}^{si} \leq P_h^{si,\max} I_{h,t}^{si} \quad \forall h, \forall t, \tag{26}$$

$$I_{h,t}^{ch} + I_{h,t}^{dis} + I_{h,t}^{si} \leq 1 \quad \forall h, \forall t, \tag{27}$$

$$GC_{h,t}^{CAES} = \frac{P_{h,t}^{dis}}{\eta_h^{dis}} + \frac{P_{h,t}^{si}}{\eta_h^{si}} \quad \forall h, \forall t. \tag{28}$$

3.1.4 | Thermal energy storage (TES)

The way in which the thermal energy is stored in TES is modelled via Equation (29), while Equation (30) declares the min/max state of storage. The initial and final state of storage is defined by Equation (31). Eventually, the nominal charge/discharge rates of TES are limited by Equations (32) and (33).

$$B_{h,t}^{HSS} = B_{h,t-1}^{HSS} + \eta_h^{ch} H_{h,t}^{ch} - \frac{H_{h,t}^{dis}}{\eta_h^{dis}} \quad \forall h, \forall t, \tag{29}$$

$$B_h^{Min} \leq B_{h,t}^{HSS} \leq B_h^{Max} \quad \forall h, \forall t, \tag{30}$$

$$B_{h,t=1}^{HSS} = B_{h,t=24}^{HSS} \quad \forall h, \forall t, \tag{31}$$

$$0 \leq H_{h,t}^{ch} \leq H_{h,Max}^{ch} \quad \forall h, \forall t, \tag{32}$$

$$0 \leq H_{h,t}^{dis} \leq H_{h,Max}^{dis} \quad \forall h, \forall t. \tag{33}$$

3.1.5 | Natural gas storage (NGS)

It is provided that the natural gas is stored in NGS according to Equation (34). The nominal charge/discharge flow rate of natural gas is restricted by Equations (35) and (36). Furthermore, the min/max storage capacity is taken to consideration by Equation (37). Similar to other storage technologies, the initial and final state of storage are equalized by Equation (38).

$$GS_{h,t}^{GSS} = GS_{h,t-1}^{GSS} + \eta_h^{GSS,ch} G_{h,t}^{ch} - \frac{G_{h,t}^{dis}}{\eta_h^{GSS,dis}} \quad \forall h, \forall t, \tag{34}$$

$$0 \leq G_{h,t}^{ch} \leq GS_h^{ch,\max} \quad \forall h, \forall t, \tag{35}$$

$$0 \leq GS_{h,t}^{dis} \leq GS_h^{dis,\max} \quad \forall h, \forall t, \tag{36}$$

$$GS_h^{Min} \leq GS_{h,t}^{GSS} \leq GS_h^{Max} \quad \forall h, \forall t, \tag{37}$$

$$GS_{h,t=0} = GS_{h,t=24} \quad \forall h, \forall t. \tag{38}$$

3.1.6 | Electrical boiler (EB)

Besides its high efficiency, EB is an effective way of converting wind power overproduction to thermal energy. Under this rationale, the EB does not only maximize wind power usage, but also enhances the flexibility in thermal energy procurement. Furthermore, it has a supportive role at the peak demand period, when the thermal output of the CHP might be insufficient. In terms of a mathematical expression, Equation (39) illustrates the thermal energy conversion of the EB, while its consumption is limited by Equation (40).

$$H_{h,t}^{EB} = \eta_h^{EB} P_{h,t}^{EB} \quad \forall h, \forall t, \tag{39}$$

$$0 \leq P_{h,s,t}^{EB} \leq P_h^{EB,\max} \quad \forall h, \forall t. \tag{40}$$

3.2 | Multi-energy equilibrium

The electrical, thermal and natural gas consumption/production equilibrium is ensured via Equations (41)–(43), respectively.

$$\begin{aligned} &P^{MES}_{h,t} + P^{CHP}_{h,t} + P^{Wind}_{h,t} + P^{ch}_{h,t} + P^{si}_{h,t} \\ &- P^{dis}_{h,t} - P^{EB}_{h,t} - P^{D}_{h,t} = 0 \forall h, \forall t, \end{aligned} \tag{41}$$

$$\begin{aligned} &H^{CHP}_{h,t} + H^{EB}_{h,t} + H^{ch}_{h,t} \forall h, \forall t \\ &- H^{dis}_{h,t} - H^{D}_{h,t} = 0, \end{aligned} \tag{42}$$

$$\begin{aligned} &G^{MES}_{h,t} + G^{dis}_{h,t} - G^{ch}_{h,t} - \left(\frac{P^{CHP}_{h,s,t}}{\eta^{CHP}_{h}} + SU_{h,t} + SD_{h,t} \right) \\ &- GC^{CAES}_{h,t} - G^{D}_{h,t} = 0 \forall h, \forall t. \end{aligned} \tag{43}$$

3.3 | Wholesale electricity market operator (individual lower-level follower)

The WEM operator receives offers/bids from Gencos, consumers and MES. At this point, the WEM operator must aggregate the offers/bids and clear the market to announce finial MCP. The process of market-clearing is defined by an optimization problem, where the objective is to maximize the social welfare (or minimize operation costs) for all market participants. More information on market-clearing and social welfare function can be found in [33] The social welfare maximization objective of the WEM is established by Equation (44), wherein the first term corresponds to the Genco power production cost, while the second term is the cost of energy MES has offered/bided to sell/purchase. The TS energy balance is declared by Equation (45), while Gencos production limits are established through Equation (46). Ramp up/down restriction of Gencos are declared by Equations (47)–(50), while Equation (51) circumscribes the purchased/sold power of MES in WEM. Equations (52) and (53) limit the power flow in TS lines and voltage angle, respectively. In power flow equations, the slack bus must always have a zero voltage angle, which is declared by Equation (54).

$$\min \left\{ \sum_{t} \sum_{g} C^{G}_{g} P^{G}_{g,t} - \sum_{t} \sum_{h} C^{MES}_{h,t} P^{MES}_{h,t} \right\}, \tag{44}$$

$$\begin{aligned} &\sum_{g \in A^{g}_{b}} P^{G}_{g,t} - \sum_{h \in A^{h}_{b}} P^{MES}_{h,t} - P^{D}_{b,t} = \\ &\sum_{b' \in Tr} B_{b,b'} (\delta_{b,t} - \delta_{b',t}) : \lambda_{b,t} \forall b, \forall t, \end{aligned} \tag{45}$$

$$0 \le P^{G}_{g,t} \le P^{GMax}_{g,t} : \mu^{G\min}_{g,t}, \mu^{G\max}_{g,t} \quad \forall g, \forall t, \tag{46}$$

$$P^{G}_{g,t} - P^{G}_{g,t-1} \le RU_{g} : \mu^{1,\min}_{g,t} \quad \forall g, \forall t > 1, \tag{47}$$

$$P^{G}_{g,t} - P^{G}_{g,ini} \le RU_{g} : \mu^{2,\min}_{g,t} \quad \forall g, \forall t = 1, \tag{48}$$

$$P^{G}_{g,t-1} - P^{G}_{g,t} \le RD_{g} : \mu^{3,\min}_{g,t} \quad \forall g, \forall t > 1, \tag{49}$$

$$P^{G}_{g,ini} - P^{G}_{g,t} \le RD_{g} : \mu^{4,\min}_{g,t} \quad \forall g, \forall t = 1, \tag{50}$$

$$\begin{aligned} &P^{MES,Min}_{t} \le P^{MES}_{h,t} \le P^{MES,Max}_{t} \\ &: \mu^{MES,\min}_{h,t}, \mu^{MES,\max}_{h,t} \forall h, \forall t \end{aligned}, \tag{51}$$

$$\begin{aligned} &-C^{Max}_{b,b'} \le B_{b,b'} (\delta_{b,t} - \delta_{b',t}) \le C^{Max}_{b,b'} \\ &: v^{\min}_{b,b',t}, v^{\max}_{b,b',t} \forall b, \forall b', \forall t \end{aligned}, \tag{52}$$

$$-\pi \le \delta_{b,t} \le \pi : \xi^{\min}_{b,t}, \xi^{\max}_{b,t} \quad \forall b, \forall t, \tag{53}$$

$$\delta_{b=ref,t} = 0 : \xi^{l}_{b=ref,t} \quad \forall b, \forall t. \tag{54}$$

3.4 | Natural gas market operator (individual lower-level follower)

Equation (55) illustrates the NGM objective that consists of two terms. The first one is the cost the gas producers, while the latter is the cost of the natural gas purchased by MES operator in NGM. The gas well production capacity is defined by Equation (56). Since the NGN is situated at the lower level, it is necessary to use the following convex model, where the nodal pressure is ignored, and the flow rate is limited. Accordingly, Equations (57) and (58) model the natural gas flow in active (with compressors) and non-active (without compressors) pipelines, respectively. The amount of natural gas that MES can exchange with NGM is restricted by Equation (59). Eventually, the natural gas consumption/production equality is defined in Equation (60).

$$\sum_{t} \left\{ \sum_{w} C^{gas}_{w} q_{w,t} - \sum_{k} C_{k,t} G^{GFU}_{k,t} \right\}, \tag{55}$$

$$0 \le q_{w,t} \le q^{\max}_{w}; \beta^{1,\max}_{w,t} \beta^{1,\min}_{w,t} \quad \forall w, \forall t, \tag{56}$$

$$-q^{\max}_{\lg} \le q_{\lg,t} \le q^{\max}_{\lg}; \beta^{2,\max}_{\lg,t} \beta^{2,\min}_{\lg,t} \quad \forall \lg, \forall t, \tag{57}$$

$$0 \le q_{c,t} \le q^{\max}_{c}; \beta^{3,\max}_{c,t} \beta^{3,\min}_{c,t} \quad \forall c, \forall t, \tag{58}$$

$$0 \le G^{MES}_{h,t} \le G^{\max}_{h}; \beta^{4,\max}_{h,t}, \beta^{4,\min}_{h,t} \quad \forall h, \forall t, \tag{59}$$

$$\begin{aligned} &\sum_{w \in A^{w}_{n}} q_{w,t} + \sum_{\{.\} \in \varphi^{+}_{n}} q_{\{.\},t} - \sum_{\{.\} \in \varphi^{-}_{n}} q_{\{.\},t} - \sum_{h \in A^{h}_{n}} G^{GFU}_{h,t} \\ &- \sum_{dg \in A^{dg}_{n}} q_{dg,t} = 0; \gamma_{n,t}\{.\} \in \{\lg, c\}, \quad \forall n, \forall t \end{aligned}. \tag{60}$$

3.5 | Information gap decision theory (IGDT)

An optimization problem can generically be expressed as follows:

$$f(x,\rho) = \min\left\{f(x,\rho)\right\}, \tag{61}$$

$$h(x,\rho) = 0, g(x,\rho) \le 0, \tag{62}$$

$$x \in Y. \tag{63}$$

Wherein the ρ is the uncertain parameter and Y is the set of uncertainties. Moreover, x represents the vector of decision variables. The uncertain parameter ρ is defined as follows [34]:

$$u(\bar{\rho},\alpha) = \left\{\rho : \left|\frac{\rho-\bar{\rho}}{\rho}\right| \le \alpha\right\}, \alpha \ge 0. \tag{64}$$

In Equation (64), $\bar{\rho}$ is the variable that entails the value for the uncertain parameter, considering the risk adjustments. α declares the maximum radius of the uncertainty considering the forecasted value. If the optimization problem was solved deterministically, it could be expressed as follows:

$$f_b^*(x,\bar{\rho}) = \min\left\{f(x,\bar{\rho})\right\}, \tag{65}$$

$$h(x,\bar{\rho}) = 0, g(x,\bar{\rho}) \le 0. \tag{66}$$

3.5.1 | Risk-averse framework

The final formulation defined in the previous subsection is risk-neutral. Therefore, the risk-averse IGDT is deployed, when the operator is willing to endure a pre-specified amount of cost to have a more robust operational schedule considering uncertain parameters. All that the IGDT approach requires is the radius of the uncertainty around the predicted (expected) value of the uncertain parameter. Overall risk-averse strategy is mathematically expressed as follows [31]:

$$\max\{\alpha\}, \tag{67}$$

$$h(\varphi,\bar{\rho}) = 0, g(\varphi,\bar{\rho}) \le 0, \tag{68}$$

$$f(\varphi,\rho) \le f_b^*(\varphi,\bar{\rho})(1+\varsigma), 0 \le \varsigma \le 1, \tag{69}$$

$$\rho = (1-\alpha)\bar{\rho}. \tag{70}$$

As can be seen, the uncertainty radius α is maximized in Equation (67) subjected to pre-defined cost value, which is specified as a ratio of the optimal cost at expected value of uncertain parameter in Equation (69). In other words, the higher the value of ς (risk adjustment parameter), the more risk-averse the operation scheduling will be. In this study, the aforementioned risk-averse strategy is deployed to handle wind power uncertainties in a robust manner. Therefore, the system is scheduled for the lower and more conservative end of the predicted wind power radius as follows:

$$\max\{\alpha\}, \tag{71}$$

$$OF_b = \{OF : \min OF\}, \tag{72}$$

$$OF \le OF_b(1+\varsigma), 0 \le \varsigma \le 1, \tag{73}$$

$$0 \le P_{b,t}^{Wind} \le (1-\alpha)\bar{P}_t^{Wind}, \tag{74}$$

subject to: Upper-level constraints: Equations (2)–(42). Lower-level constraints: Equations (45), (54), and (60).

3.5.2 | Risk-seeker framework

In a risk-seeker strategy the operator is optimistic that the value of uncertain parameter will take values that decrease the cost function. Therefore, the operator opportunistically bets on the value of the uncertain parameter, hoping to gain higher profit. The risk-seeker model is expressed as follows [31]:

$$\min\{\alpha\}, \tag{75}$$

$$h(\varphi,\bar{\rho}) = 0, g(\varphi,\bar{\rho}) \le 0, \tag{76}$$

$$f(\varphi,\rho) \le f_b^*(\varphi,\bar{\rho})(1-\beta), 0 \le \beta \le 1, \tag{77}$$

$$\rho = (1+\alpha)\bar{\rho}. \tag{78}$$

In Equation (75), the main objective is to minimize the uncertainty radius to gain lower cost values, which is defined by β (opportunity adjustment parameter). In this study, this risk-seeker strategy is deployed to handle wind power uncertainty in an opportunistic manner that might lead to higher profit for the MES operator. Therefore, the operation is conducted considering that the uncertain parameter might take values that are in favor of the MES operator. Overall, this strategy is established by the following equations:

$$\min\{\alpha\}, \tag{79}$$

$$OF_b = \{OF : \min OF\}, \tag{80}$$

$$OF \le OF_b(1-\beta), 0 \le \beta \le 1, \tag{81}$$

$$0 \le P_{b,t}^{Wind} \le (1+\alpha)\bar{P}_t^{Wind}. \tag{82}$$

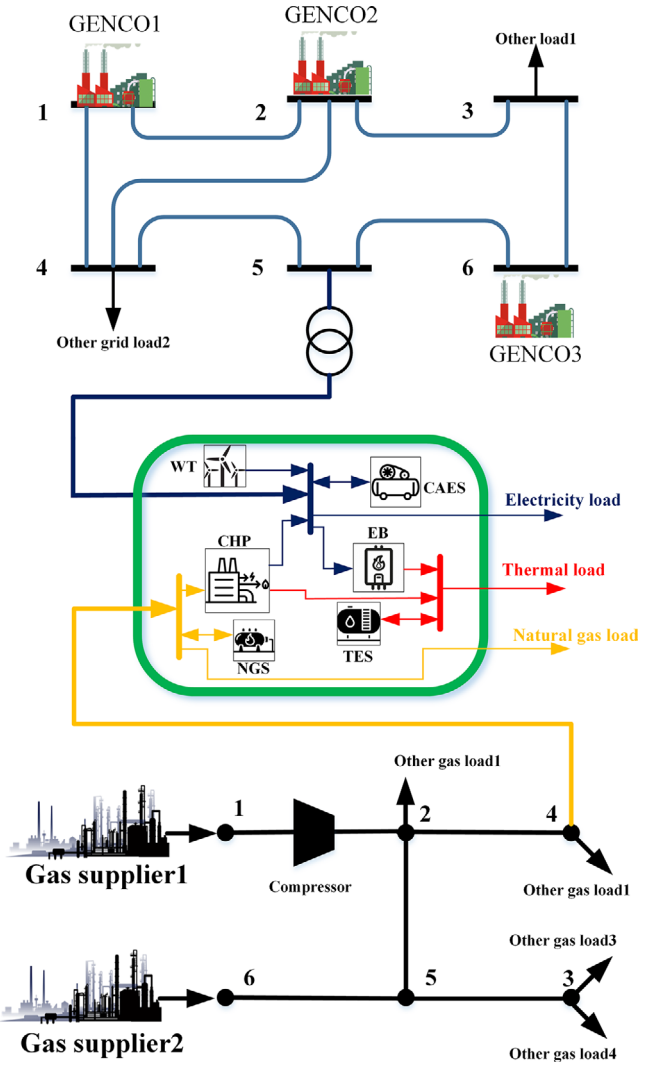

FIGURE 4 The overall schematic of the systems, connections, and nodal locations

4 | CASE STUDIES AND RESULTS

In this study, the WEM and NGM are established through standard 6-bus TS and 6-node NGN, respectively. The TS includes three Gencos, two load nodes, and seven transmission lines. The NGN entails two gas wells, six pipelines and four load points. The technical data on TS and NGN can be extracted from [35]. Overall configuration of the systems and connections of MES with NGN/WEM is illustrated by Figure 4. The forecasted electrical, thermal and natural gas demands of MES is observable in Figure 5. More information on equipment utilized in MES are included in Appendix A. The proposed MILP was solved with a standard CPLEX solver under the following case studies (CS):

- **CS1**: The tactical behavior of the MES, as a price setter, in the NGM and WEM is evaluated ignoring the existence of MCESs.

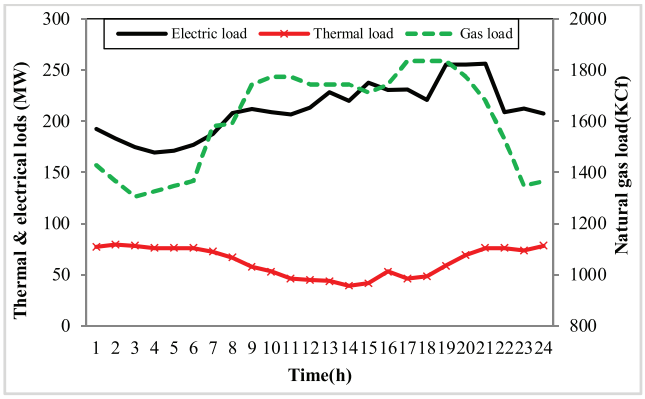

FIGURE 5 Forecasted electrical, thermal and natural gas demands of MES

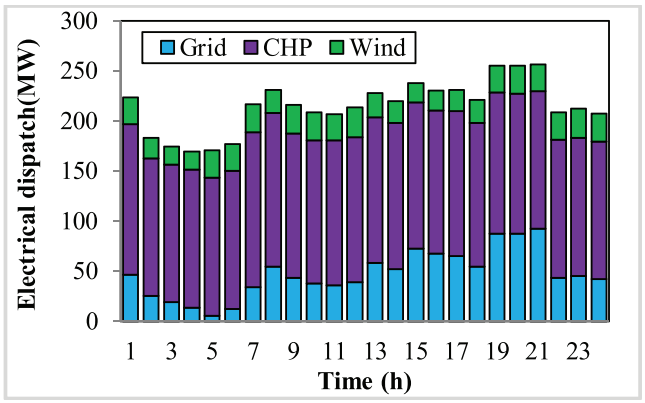

FIGURE 6 Hourly electrical dispatch scheduling in **CS1**

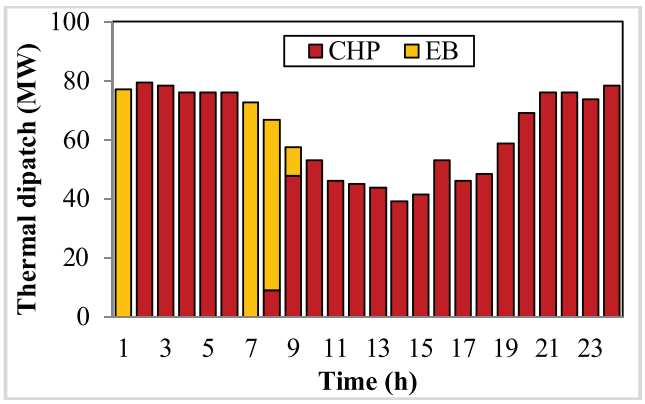

FIGURE 7 Hourly thermal dispatch to supply demand in **CS1**

- **CS2**: The tactical behavior of the MES, as a price-setter, in the NGM and WEM is evaluated considering MCESs.
- **CS3**: The IGDT framework is added to the **CS2**.

CS1: In this case, the MES is tactically scheduled while neglecting the MCESs. The hourly thermal and electrical dispatch scheduling of this case is illustrated in Figures 6 and 7. Based on the obtained results, the CHP supplies the highest

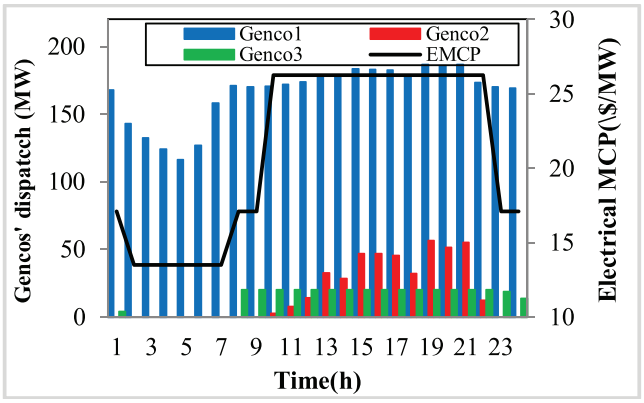

FIGURE 8 Hourly Genco commitment scheduling and EMCP in **CS1**

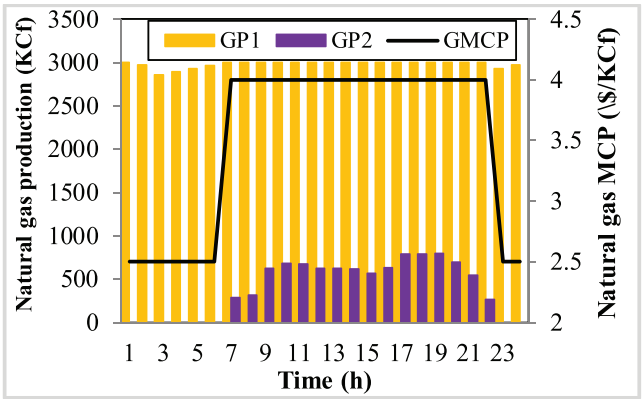

FIGURE 9 Hourly gas production scheduling and GMCP in **CS1**

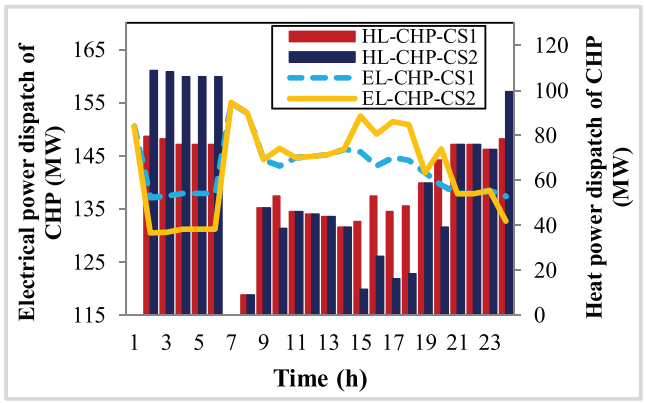

FIGURE 10 Thermal/electrical dispatch scheduling of the CHP unit in **CS2**

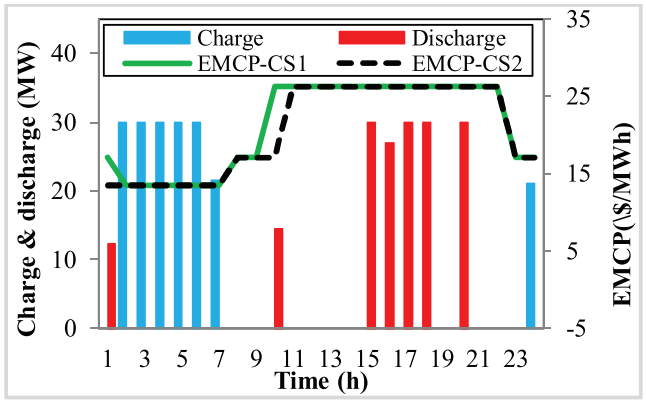

FIGURE 11 Absorbed/released thermal energy of the TES and EMCP in **CS2**

portion of the load with 3425.38 MWh production. Moreover, WEM and WT account for 1134.06 MWh and 596.43 MWh of the demand. Figure 8 illustrates the MCP and hourly scheduling of the Gencos. As can be observed, at the early hours of the day (hours 2–7), when the demand is low, expensive gencos are not operative. Therefore, the MCP is as low as 13.5 \$/MWh. With a relative rise in demand during hours 8–9, Genco3 is started, which increases MCP up to 17.5 \$/MWh. To account for the high MES demand at hours 10–22, Genco2 (high-cost unit) is activated, which raises MCP up to 26.25 \$/MWh. However, with the shutdown of Genco2 at hour 22, the MCP drops back to 17.1 \$/MWh. The hourly scheduling of natural gas suppliers and MCP of NGM is illustrated by Figure 9. As can be seen, during off-peak periods (hours 1–6), the natural gas demand is supplied with the cheaper units, which leads to the MCP of 2.5 \$/KCf. Nonetheless, the upsurge in demand during the hours 7-22 is satisfied through more expensive suppliers that elevate the MCP up to 4 \$/MWh. That said, after hour 22, the natural gas demand transcends its peak value, thereby decreasing to 2.5 \$/KCf.

CS2: In this case, the tactical scheduling of the MES in WEM and NGM is evaluated with the inclusion of the MCES.

- The influence of TES on the tactical behavior of the MES: Figure 10 illustrates the influence of TES on thermal/electrical dispatch scheduling of the CHP unit. In this figure, the line graph and the bar chart illustrate the electrical and thermal production of the CHP. Moreover, Figure 11 depicts the absorbed/released thermal energy of the TES. Based on these findings, the TES is scheduled to absorb thermal energy at hours 2–7, which is the reason for this higher thermal dispatch of the CHP at these hours compared to **CS1**. With the release of thermal energy at hours 11 and 15–21, the thermal CHP dispatch is declined. Considering that the operation of the CHP is confined to FOR, the thermal and electrical output of the CHP are interdependent decision variables. Therefore, increasing the thermal output at hours 2–7 has led to lower electrical dispatch. On the other hand, with the higher thermal dispatch at hours 11 and 15–21, the electrical output is enhanced. The charge/discharge scheduling of the TES and MCP of WEM is illustrated in Figure 11. Notably, the inclusion of TES leads to 2.51% lower MCP compared to **CS1**.
- The influence of the CAES on the tactical behavior of the MES: In Figure 12, the bar chart represents the charge/discharge schedule of the CAES, while the state of charge (SOC) is depicted by the line graph. Based on the results, the CAES stores compressed air energy at off-peak

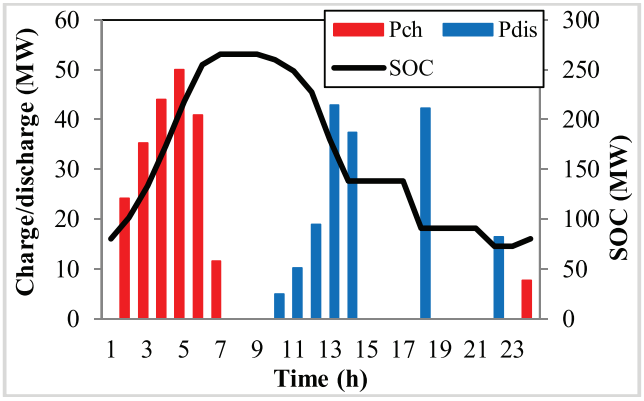

FIGURE 12 Hourly scheduling charge/discharge of the CAES in **CS2**

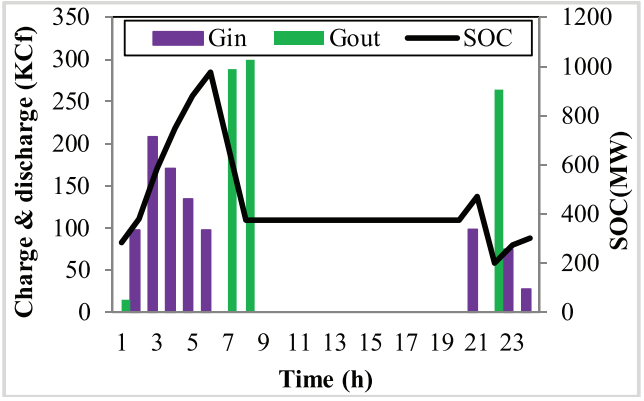

FIGURE 14 The state of NGS and stored/released natural gas in **CS2**

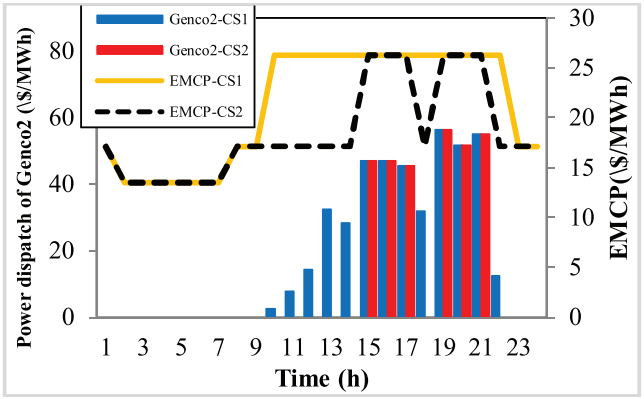

FIGURE 13 MCP of WEM and hourly scheduling of Genco2 in **CS2**

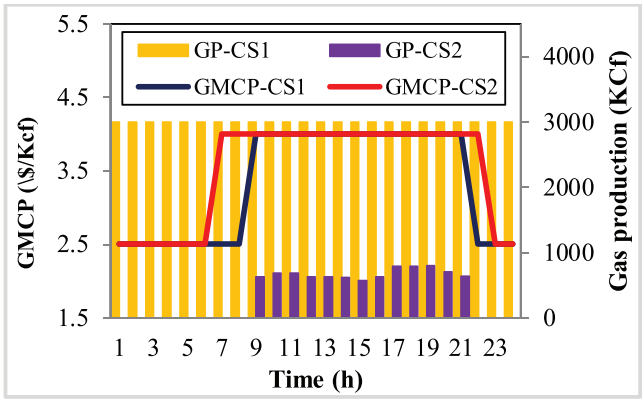

FIGURE 15 Hourly scheduling gas produced and GMCP in **CS2**

intervals, and releases it back at expensive market periods. The line graph and bar chart in Figure 13 illustrate the MCP of WEM and hourly scheduling of Genco2 (high-cost unit), respectively. Accordingly, with the integration of the CAES in **CS2**, the energy is procured at cheaper market hours, thereby leading to lower Genco2 (expensive unit) dispatch (compared to **CS1**) and 12.61% lower MCP in WEM.

- The influence of NGS on the tactical behavior of the MES: The state of NGS and stored/released natural gas in NGS is illustrated by Figure 14. Additionally, the MCP of NGM in **CS1** and **CS2** are compared in Figure 15. It is noteworthy that the natural gas is released during hours 7–9 and 22, and it has decreased the MCP of NGM compared to **CS1**.
- The influence of NGS on the tactical behavior of the MES: in this subcase, all of the three storage technologies (TES, CAES and NGS) are taken into consideration. The MCP of WEM and NGM in **CS1** and **CS2** are plotted in Figures 16 and 17, respectively. Based on these figures, the incorporation of MCESs can bring down the MCP of WEM by 13.32%. Furthermore, the MCP of NGM is reduced by 5.36%. In other words, during hours 10–14, 18, 22, the MES has become a price setter market player in WEM, and it is a price setter player in NGM during hours 8–9, 22. Table 2 summarizes various operational costs and the cost of participating in WEM/NGM. As can be seen, the previous hypothesis on the

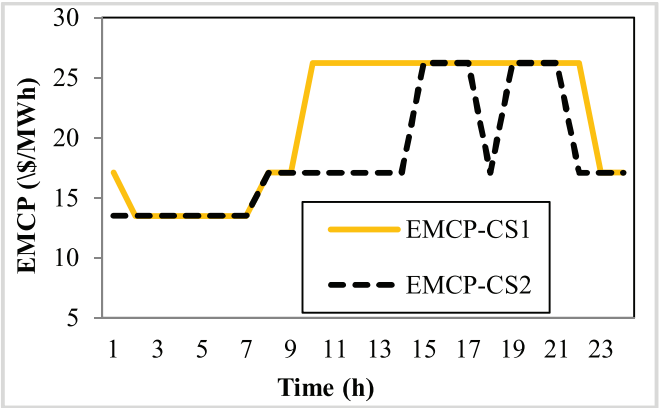

FIGURE 16 Hourly scheduling MCP of WEM in **CS2**

effect of MCES is further substantiated since the cost values have experienced a dramatic reduction.

CS3: In this case, the impact of integration MCES is evaluated considering the uncertainties driven by wind power. In this regard, the risk-averse and risk-seeker IGDT frameworks are deployed. The risk-averse strategy is scrutinized in Table 3, wherein the risk control parameter (ζ) is increased by step-width of 0.005, from 0 to 0.02, which shows the

TABLE 2 The effect of multi-carrier energy storage systems in the operational costs of multi-energy system

Storage systems	CS1	CS1+TES	CS1+CAES	CS1+NGS	CS1+TES+ CAES+NGS
Power purchased from the EWM	26257.01	25407.485	23270.53	27557.21	23291.28713
Gas purchased from the GWM	192541	192344.02	193327.2	182049.6	183148.4279
HSS costs	0	86.90071	0	0	98.36862931
CAES costs	0	0	1161.042	0	1708.864881
GSS Cost	0	0	0	272.5717	267.5221976
Total operation costs	218798	217838.41	217758.8	209879.4	208514.4708

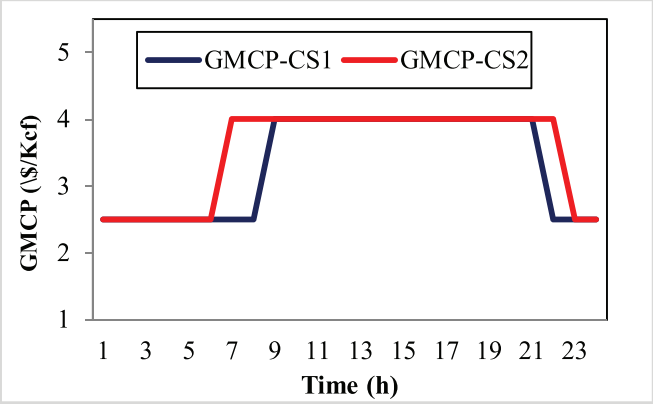

FIGURE 17 Hourly scheduling MCP of NGM in **CS2**

TABLE 3 Total cost and uncertainty radius in different operational modes of risk-averse scheduling

Total operation cost	$\zeta = 0.00$	$\zeta = 0.005$	$\zeta = 0.010$	$\zeta = 0.015$	$\zeta = 0.020$
Without MCSS	218798	219910.41	220604.4	221425.04	221425
With HSS	217838.4	218926.92	219880.6	220629.58	221711.1
With CAES	217758.8	218865.83	219527.7	220632.02	221299.1
With GSS	209879.4	210937.15	211531.1	212378.14	213424.6
With MCES	208514.5	209134.3	209749.9	210798.96	211843.6
a	$\zeta = 0.00$	$\zeta = 0.005$	$\zeta = 0.010$	$\zeta = 0.015$	$\zeta = 0.020$
Without MCSS	0	0.056001	0.061018	0.1379684	0.137968
With HSS	0	0.0816969	0.124055	0.1743708	0.253163
With CAES	0	0.0610176	0.125567	0.1947832	0.257533
With GSS	0	0.056001	0.061018	0.1255155	0.202815
With MCES	0	0.0614252	0.121088	0.18027	0.23977

impact that risk-averse strategy can impose. As can be seen, increasing ζ leads to a higher uncertainty radius (a), which makes the operation scheduling more reliable and robust, while imposing higher overall operational costs for MES operator. It is noted that when MCESs are included, the value of a is higher, which illustrates how the MCESs can be helpful in risk-aversion since for the same amount of cost a higher uncertainty radius is achieved. Moreover, the influence of ζ on other important decision variables is illustrated in Table 4. For instance, when $\zeta = 0.02$, the power purchased from WEM and MCP of WEM is dropped by 11.84% and 4.159%, respectively. Nevertheless, the influence on some decision variables, such as power production of Genco3 and MCP of NGM is insignificant.

TABLE 4 Impact of uncertainty on the important decision variables in risk-averse approach

	$\zeta = 0.00$	$\zeta = 0.005$	$\zeta = 0.010$	$\zeta = 0.015$	$\zeta = 0.020$
$\sum_{h,t} P^{Wind}_{h,t}$	596.4371	559.8008	524.2156	488.9174	453.4295
$\sum_{g,t} P^{G}_{g=1,t}$	4149.022	4161.602	4174.971	4178.822	4183.328
$\sum_{g,t} P^{G}_{g=2,t}$	308.3225	346.9572	388.0114	399.8384	413.6752
$\sum_{g,t} P^{G}_{g=3,t}$	340	340	340	340	340
$\sum_{h,t} P^{MES}_{h,t}$	1179.959	1231.174	1285.597	1301.275	1319.618
$\sum_{h,t} G^{MES}_{h,t}$	54079.84	54020.34	53944.74	54007.76	54038.27
$\sum_{i,t} \lambda_{i=5,t}$	440.12	449.2733	458.4267	458.4267	458.4267
$\sum_{n,t} \gamma_{n=5,t}$	79.5	79.5	79.5	79.5	79.5

To scrutinize the influence of the risk-seeker approach on the MES, a sensitivity analysis is conducted in Table 5 on opportunity control parameter (β) with a step-width of 0.005 from 0 to 0.02. As illustrated, a higher opportunity control parameter (β) leads to a higher uncertainty radius (a). For instance, when $\beta = 0.02$ the values of $a = 0.274$ without MCESs, while $a = 0.261$ with MCESs. In other words, when the storage technologies are involved in MES, the same amount of opportunity can be achieved with lower β. In addition, other essential decision variables have been summarized in Table 6 for different opportunity function values. Based on these values, increasing the value of β up to 0.02 can reduce the purchased energy from WEM by 5.82% and MCP of WEM by 0.83%. However, the influence on other decision variables, such as the production of Genco3 or MCP of the NGM is insignificant.

TABLE 5 Total cost and uncertainty radius in different operational modes of risk-seeker scheduling

Total operation cost	$\beta = 0.00$	$\beta = 0.005$	$\beta = 0.01$	$\beta = 0.015$	$\beta = 0.020$
Without MCES	218798	217701.1	216939.7	215972.6	214872.2
With HSS	217838.4	216749.3	215126.1	214378.4	213289.6
With CAES	217758.8	216129.9	215158.3	214266.2	213386.2
With GSS	209879.4	208827.5	208111.4	207373.5	206319.6
With MCES	208514.5	207462.2	206407.8	205343.8	204427.4
a	$\beta = 0.00$	$\beta = 0.005$	$\beta = 0.01$	$\beta = 0.015$	$\beta = 0.020$
Without MCES	0	0.085708	0.12077	0.187303	0.273883
With HSS	0	0.08525	0.121211	0.161127	0.246398
With CAES	0	0.074056	0.135764	0.187303	0.259338
With GSS	0	0.081488	0.116439	0.158699	0.215141
With MCES	0	0.061259	0.124927	0.19275	0.260919

TABLE 6 Impact of uncertainty on the important decision variables in risk seeker approach

	$\beta = 0.00$	$\beta = 0.005$	$\beta = 0.01$	$\beta = 0.015$	$\beta = 0.020$
$\sum_{h,t} P_{h,t}^{Wind}$	596.4371	632.9742	670.9485	711.4001	752.059
$\sum_{g,t} P_{g=1,t}^{G}$	4149.022	4145.639	4142.565	4140.9	4133.52
$\sum_{g,t} P_{g=2,t}^{G}$	308.3225	297.9347	288.4954	283.3815	275.0773
$\sum_{g,t} P_{g=3,t}^{G}$	340	340	340	340	320
$\sum_{h,t} P_{h,t}^{MES}$	1179.959	1166.188	1153.675	1146.896	1111.212
$\sum_{h,t} G_{h,t}^{MES}$	54079.84	54043.46	53967.21	53766.48	53739.09
$\sum_{i,t} \lambda_{i=5,t}$	440.12	440.12	440.12	440.1198	436.52
$\sum_{n,t} \gamma_{n=5,t}$	79.5	79.5	79.5	79.5	79.5

5 | CONCLUSION

In this study, the tactical scheduling of a wind farm-integrated MES in WEM and NGM as a price-setter was proposed under a bi-level multi-follower optimization approach. The WEM and NGM were considered as individual followers, while modelling MES as the upper-level leader. The MES was equipped with MCESs, such as TES, NGS and CAES, and its objective was to reduce total operational costs and the cost of taking part in WEM and NGM as a price setter. On the other hand, the objective of WEM and NGM was to maximize public satisfaction. To solve the bi-level nonlinear problem, the theory of strong duality and KKT conditions were deployed, which transformed it into single-level conventional MILP. Moreover, IGDT was applied to the wind power uncertainty under both risk-averse and risk-seeker frameworks. Eventually, the study was expanded to various case studies to study its practicality. Overall, the following conclusive points were drawn:

1. The participation of MES in WEM and NGM, as a price-setter with a CAES, can bring down the overall cost by 0.474% while diminishing electrical MCP by 12.61%.
2. Including TES in the MES does not only bring down the electrical MCP by 2.5%, but it also enhances the flexibility of the CHP at peak and expensive periods.
3. Integration of NGS in the MES, as a price-setter player leads to 5.35% reduction in natural gas MCP.
4. When the MCESs were incorporated in the price-setter MES, the total operational cost was decreased by 4.7%, while diminishing the electrical and natural gas MCP by 13.32% and 5.53%, respectively.
5. The IGDT approach gives the MES operator a tool to evaluate the influence of the wind power uncertainty when participating in the WEM and NGM. The operator can choose between risk-averse and risk-seeker strategies.

CONFLICT OF INTEREST

The authors have declared no conflict of interest.

DATA AVAILABILITY STATEMENT

Data available in article supplementary material.

NOMENCLATURE

Abbreviations

WT	wind turbine
MES	Multi-energy system
WEM	Wholesale electricity market
NGM	Natural gas market
TES	Thermal energy storage
CAES	Compressed air energy storage
NGS	Natural gas storage
MCP	Market-clearing price
KKT	Karush-Kuhn-Tucker
IGDT	Information gap decision theory
TS	Transmission system
NGN	Natural gas network
CHP	Combined heat and power
Genco	Generation company
EB	Electrical boiler

Sets and indices

t, h	Indices of time period, MES
b, n	Indices of power system bus's, natural gas nods
R	Indices of feasible operation region
g, w	Indices of Genco's, gas producer
lg, c	Indices of non-active, active natural gas pipelines
A_n^m	Set of m equipment's located at TS bus's or NGN nodes n Tr Set of power system brunch

Parameters

$C_{h,t}^{cb}, C_{h,t}^{dis}, C_{h,t}^{si}$	Charge/discharge/simple cycle costs of CAES($/MWh)
$C_{h,t}^{out}, C_{h,t}^{Hdis}$	Discharge cost of NGS and TES ($/MWh)

P^R, H^R Power/heat generation in feasible operation region of CHP (MW)

γ_p, γ_H Power/heat conversion factors of CHP for converting gas to electrical and thermal energy (MW)

C_b^{SU}, C_b^{SD} Coefficients of fuel used to startup and shutdown the CHP units (Kcf)

R_b^{UP}/R_b^{DN} Ramp up/down limits of the CHP (MW)

T_b^U, T_b^D Minimum up and down times of the CHP (h)

$T_b^U e, T_b^D e$ Minimum up and down times in the beginning of the study horizon (h)

$\eta_b^{ch}, \eta_b^{dis}, \eta_b^{si}$ Charge/discharge/simple cycle efficiency of the CAES (%)

$E_{b,t}^{\min}, E_{b,t}^{\max}$ Minimum/maximum storage capacity of the CAES (MW)

$P_b^{ch,\min}, P_b^{ch,\max}$ Minimum/maximum charge rate of the CAES (MW)

$P_b^{dis,\min}, P_b^{dis,\max}$ Minimum/maximum discharge rate of CAES (MW)

$E_{b,t=24}^{\min}, E_{b,t=1}^{\min}$ Initial and final values of stored energy in the CAES (MW)

$\eta_b^{ch}, \eta_b^{dis}$ Charge/discharge efficiency of the TES (%)

B_b^{Min}, B_b^{Max} Minimum/maximum storage capacity of the TES (MW)

$H_{b,Max}^{ch}, H_{b,Max}^{dis}$ Maximum charge/discharge rate of TES (MW)

$B_{b,t=1}^{HSS}, B_{b,t=24}^{HSS}$ Initial and final storage state of TES (MW)

$\eta_b^{GSS,ch}, \eta_b^{GSS,dis}$ Charge/discharge efficiency of NGS (%)

GS_b^{Min}, GS_b^{Max} Minimum/maximum storage capacity of NGS (KCf)

$\overline{GS_b^{ch}}, \overline{GS_b^{dis}}$ Maximum charge/discharge rate of NGS (KCf)

η_b^{EB} Conversion factor of EB to convert electrical power to thermal energy(MW)

$P_b^{EB,\max}$ Maximum thermal power generation rate of EB (MW)

$P_{b,t}^D, H_{b,t}^D, G_{b,t}^D$ forecasted electrical/thermal/gas loads of MES (MW)

C_g^G Offered price of Gencos in WEM ($/MWh)

C_w^{gas} Offered price of gas producer in NGM ($/KCf)

$P_{g,t}^{GMax}, C_{b,b'}^{Max}$ Maximum power generation limit of Gencos (MW)

RU_g, RD_g Ramp up/down limits of Gencos (MW)

$P_t^{MES,Min}, P_t^{MES,Max}$ Minimum/maximum power exchanged between MES and WEM .NGM (MW)

$C_{b,b'}^{Max}$ Maximum transferable power from the power transmission lines (MW)

$q_w^{\max}, G_b^{\max}$ Maximum gas producer limit, maximum limit of the gas purchased by the MES (KCf)

$q_{\lg}^{\max}, q_c^{\max}$ Maximum transferable gas from the non-active and active pipeline (KCf)

$P_{b,t}^D, q_{dg,t}$ Forecasted electrical and gas loads in power system and natural gas system

Variables

OF Leader's objective function

$P_{b,t}^{MES}, G_{b,t}^{MES}$ Amount of electricity and gas exchanged between MES and WEM .NGM

$P_{b,t}^{CHP}, H_{b,t}^{CHP}$ Amount of electricity and heat generated of the CHP unit (MW)

$Q_{b,t}^{CHP}$ Amount of gas consumed by CHP unit (KCf)

$SU_{b,t}, SD_{b,t}$ Amount of fuel gas consumed by the CHP unit to Startup/shutdown (Kcf).

α_t^R Combination coefficient of corner points

$E_{b,t}^{CAES}, B_{b,t}^{HSS}$ Amount of stored energy in CAES and TES (MW)

$GS_{b,t}^{GSS}$ Amount of stored gas in NGS (KCf)

$P_{b,t}^{ch}, P_{b,t}^{dis}, P_{b,t}^{si}$ Amount of charge/discharge/simple cycle of the CAES (MW)

$GC_{b,t}^{CAES}$ Amount of gas consumed by CAES (KCf)

$H_{b,t}^{ch}, H_{b,t}^{dis}$ Charge/discharge rate of the TES (MW)

$G_{b,t}^{ch}, G_{b,t}^{dis}$ Charge/discharge rate of the NGS (KCf)

$H_{b,t}^{EB}, P_{b,t}^{EB}$ Amount of heat generated by EB, amount of electricity consumed by EB(MW)

$P_{b,t}^{Wind}$ Amount of electricity generated through wind turbine (MW)

$P_{g,t}^G$ Amount of electricity generated through Gencos (MW)

$\delta_{b,t}$ Bus's voltage angles in power system (MW)

$C_{b,t}^{MES}$ Offer/bid of the MES in the WEM ($/MWh)

$C_{k,t}$ Bid of the MES in the NGM ($/KCf)

$q_{w,t}$ Amount of gas produced of gas wells (KCf)

$q_{\lg,t}, q_{c,t}$ Amount of transferable gas at the non-active, active pipeline (KCf)

Dual variables

μ, ν, ξ Lagrange coefficients associated with inequality constraints in WEM

λ Lagrange coefficients associated with equality constraints in WEM

β Lagrange coefficients associated with inequality constraints in NGM

γ Lagrange coefficients associated with equality constraints in NGM

Binary variables

$I_{b,t}$ Commitment state of CHP.

$y_{b,t}, z_{b,t}$ Startup / shutdown state of CHP.

$I_{b,t}^{ch}, I_{b,t}^{dis}, I_{b,t}^{si}$ Charge / discharge / simple cycle states in CAES

ORCID

Sajad Najafi Ravadanegh https://orcid.org/0000-0002-9468-9990

Mousa Marzband https://orcid.org/0000-0003-3482-609X

REFERENCES

1. Davoudi, M., Moeini Aghtaie, M., Ghorani, R.: Developing a new framework for transactive peer-to-peer thermal energy market. IET Gener. Transm. Distrib. (2021)
2. Banaei, M., Oloomi buygi, M., Raouf Sheybani, H., Khooban, M.H.: Mixed supply function-cournot equilibrium model of futures and day-ahead electricity markets. IET Gener. Transm. Distrib. 15(10), 1640–1654 (2021)
3. Dong, F., Li, W., Ji, Z., Fatema, S.: Bidding strategy of thermal power compound differential evolution game under the market mechanism of peak regulation auxiliary service. IET Gener. Transm. Distrib. 15(12), 1871–1883 (2021)
4. Jiang, C., Yang, H.: Carbon tax or sustainable aviation fuel quota. Energy Econ. 103, 105570 (2021). https://www.sciencedirect.com/science/article/pii/S0140988321004424
5. Cai, J., Xu, Q.: Capacity value evaluation of wind farms considering the correlation between wind power output and load. IET Gener. Transm. Distrib. 15(9), 1486–1500 (2021)
6. Morales España, G., Nycander, E., Sijm, J.: Reducing co2 emissions by curtailing renewables: Examples from optimal power system operation. Energy Econ. 99, 105277 (2021)
7. Zhang, X., Wang, X.: Hybrid-adaptive differential evolution with decay function applied to transmission network expansion planning with renewable energy resources generation. IET Gener. Transm. Distrib. (2021)
8. Cui, Y., He, Y., Xiong, X., Chen, Z., Li, F., Xu, T., et al.: Algorithm for identifying wind power ramp events via novel improved dynamic swinging door. Renew. Energy 171, 542–556 (2021)
9. Mohammadi, M., Noorollahi, Y., Mohammadi ivatloo, B., Hosseinzadeh, M., Yousefi, H., Khorasani, S.T.: Optimal management of energy hubs and smart energy hubs - A review. Renew. Sustain. Energy Rev. 89, 33–50 (2018)
10. Moeini Aghtaie, M., Farzin, H., Fotuhi Firuzabad, M., Amrollahi, R.: Generalized analytical approach to assess reliability of renewable-based energy hubs. IEEE Trans. Power Syst. 32(1), 368–377 (2017)
11. Eladl, A.A., El Afifi, M.I., Saeed, M.A., El Saadawi, M.M.: Optimal operation of energy hubs integrated with renewable energy sources and storage devices considering CO_2 emissions. Int. J. Electr. Power Energy Syst. 117, 105719 (2020)
12. Wang, Y., Cheng, J., Zhang, N., Kang, C.: Automatic and linearized modeling of energy hub and its flexibility analysis. Appl. Energy 211, 705–714 (2018)
13. Yan, M., He, Y., Shahidehpour, M., Ai, X., Li, Z., Wen, J.: Coordinated regional-district operation of integrated energy systems for resilience enhancement in natural disasters. IEEE Trans. Smart Grid 10(5), 4881–4892 (2018)
14. Mirzaei, M.A., Oskouei, M.Z., Mohammadi Ivatloo, B., Loni, A., Zare, K., Marzband, M., et al.: Integrated energy hub system based on power-to-gas and compressed air energy storage technologies in the presence of multiple shiftable loads. IET Gener. Transm. Distrib. 14(13), 2510–2519 (2020)
15. Zhao, T., Pan, X., Yao, S., Ju, C., Li, L.: Strategic bidding of hybrid ac/dc microgrid embedded energy hubs: A two-stage chance constrained stochastic programming approach. IEEE Trans. Sustain. Energy 11(1), 116–125 (2020)
16. Najafi, A., Tavakoli, A., Pourakbari Kasmaei, M., Lehtonen, M.: A risk-based optimal self-scheduling of smart energy hub in the day-ahead and regulation markets. J. Cleaner Prod. 279, 123631 (2021)
17. Zare Oskouei, M., Mirzaei, M.A., Mohammadi Ivatloo, B., Shafiee, M., Marzband, M., Anvari Moghaddam, A.: A hybrid robust-stochastic approach to evaluate the profit of a multi-energy retailer in tri-layer energy markets. Energy 214, 118948 (2021)
18. Zare Oskouei, M., Mohammadi ivatloo, B., Abapour, M., Shafiee, M., Anvari Moghaddam, A.: Strategic operation of a virtual energy hub with the provision of advanced ancillary services in industrial parks. IEEE Trans. Sustain. Energy 12(4), 2062–2073 (2021)
19. Khorasany, M., Najafi Ghalelou, A., Razzaghi, R., Mohammadi Ivatloo, B.: Transactive energy framework for optimal energy management of multi-carrier energy hubs under local electrical, thermal, and cooling market constraints. Int. J. Electr. Power Energy Syst. 129, 106803 (2021)
20. Jadidbonab, M., Mohammadi Ivatloo, B., Marzband, M., Siano, P.: Short-term self-scheduling of virtual energy hub plant within thermal energy market. IEEE Trans. Ind. Electron. 68(4), 3124–3136 (2021)
21. Mirzapour kamanaj, A., Majidi, M., Zare, K., Kazemzadeh, R.: Electrical power and energy systems optimal strategic coordination of distribution networks and interconnected energy hubs: A linear multi-follower bi-level optimization model. Electr. Power Energy Syst. 119(February), 105925 (2020)
22. Li, R., Wei, W., Mei, S., Hu, Q., Wu, Q.: Participation of an energy hub in electricity and heat distribution markets: An mpec approach. IEEE Trans. Smart Grid 10(4), 3641–3653 (2019)
23. Yazdani Damavandi, M., Neyestani, N., Shafie khah, M., Contreras, J., Catalao, J.P.S.: Strategic behavior of multi-energy players in electricity markets as aggregators of demand side resources using a bi-level approach. IEEE Trans. Power Syst. 33(1), 397–411 (2017)
24. Najafi, A., Falaghi, H., Contreras, J., Ramezani, M.: A stochastic bilevel model for the energy hub manager problem. IEEE Trans. Smart Grid 8(5), 2394–2404 (2017)
25. Nasiri, N., Sadeghi Yazdankhah, A., Mirzaei, M.A., Loni, A., Mohammadi Ivatloo, B., Zare, K., et al.: A bi-level market-clearing for coordinated regional-local multi-carrier systems in presence of energy storage technologies. Sustain. Cities Soc. 63, 102439 (2020)
26. Khazeni, S., Sheikhi, A., Rayati, M., Soleymani, S., Ranjbar, A.M.: Retail market equilibrium in multicarrier energy systems: A game theoretical approach. IEEE Syst. J. 13(1), 738–747 (2019)
27. Nasiri, N., Zeynali, S., Ravadanegh, S.N., Rostami, N.: A robust decision framework for strategic behaviour of integrated energy service provider with embedded natural gas and power systems in day-ahead wholesale market. IET Gener. Transm. Distrib. (2021)
28. Zeynali, S., Rostami, N., Ahmadian, A., Elkamel, A.: Robust multi-objective thermal and electrical energy hub management integrating hybrid battery-compressed air energy storage systems and plug-in-electric-vehicle-based demand response. J. Storage Mater. 35, 102265 (2021)
29. Nojavan, S., Akbari Dibavar, A., Zare, K.: Optimal energy management of compressed air energy storage in day-ahead and real-time energy markets. IET Gener. Transm. Distrib. 13(16), 3673–3679 (2019)
30. Cai, W., Mohammaditab, R., Fathi, G., Wakil, K., Ebadi, A.G., Ghadimi, N.: Optimal bidding and offering strategies of compressed air energy storage: A hybrid robust-stochastic approach. Renew. Energy 143, 1–8 (2019)
31. Mirzaei, M.A., Heris, M.N., Zare, K., Mohammadi ivatloo, B., Marzband, M., Asadi, S., et al.: Evaluating the impact of multi-carrier energy storage systems in optimal operation of integrated electricity, gas and district heating networks. Appl. Therm. Eng. 176, 115413 (2020)
32. Jadidbonab, M., Babaei, E., Mohammadi ivatloo, B.: Cvar-constrained scheduling strategy for smart multi carrier energy hub considering demand response and compressed air energy storage. Energy 174, 1238–1250 (2019)
33. Conejo, A.J., Baringo, L.: Self-scheduling and market clearing auction. In: Power System Operations, pp. 233–260. Springer, Cham (2018)
34. Sheikhahmadi, P., Bahramara, S., Mazza, A., Chicco, G., Catalão, J.P.S.: Bi-level optimization model for the coordination between transmission and distribution systems interacting with local energy markets. Int. J. Electr. Power Energy Syst. 124, 106392 (2021)
35. Alabdulwahab, A., Abusorrah, A., Zhang, X., Shahidehpour, M.: Stochastic security-constrained scheduling of coordinated electricity and natural gas infrastructures. IEEE Syst. J. 11(3), 1674–1683 (2017)

How to cite this article: Nasiri, N., Zeynali, S., Najafi Ravadanegh, S., Marzband, M.: A tactical scheduling framework for wind farm-integrated multi-energy systems to take part in natural gas and wholesale electricity markets as a price setter. IET Gener. Transm. Distrib. 1–16 (2022). https://doi.org/10.1049/gtd2.12423

APPENDIX A: SUMMERY OF EQUIPMENT DATA

The data concerning the equipment in the proposed model are summarised in Table A.1.

TABLE A.1 Equipment data

Equipment	Parameter	Value
CHP unit	T_b^{U0}, T_b^{D0}	1(h)
	$I_{b,t=0}$	1
	R_b^{up}/R_b^{dn}	40 MW/40 MW
	C_b^{SU}/C_b^{SD}	3.41 K
	T_b^{Ue}/T_b^{De}	1(h)/1(h)
	γ_p, γ_H	2.41,0.31
TES	B_b^{Max}/B_b^{Min}	180 MW/10 MW
	$H_{b,Max}^{ch}/H_{b,Max}^{dis}$	30 MW/30 MW
	η_b^{ch}/η_b^{dis}	0.95 / 0.95
	$B_{b,s,t=1}^{Max}/B_{b,s,t=24}^{Min}$	30 MW
MES	$P_b^{EH,Max}/P_b^{EH,Min}$	150 MW /−150 MW
	$G_b^{\max}$	1500(KCf)
CAES	$E_{b,t}^{\min}/E_{b,t}^{\max}$	20 MW/350 MW
	$E_{b,t=24}^{\min}/E_{b,t=1}^{\min}$	80 MW
	$P_b^{ch,\min}/P_b^{ch,\max}$	5 MW/50 MW
	$P_b^{dis,\min}/P_b^{dis,\max}$	5 MW/50 MW
	$\eta_b^{ch}, \eta_b^{dis}, \eta_b^{si}$	0.9/0.9/0.4
NGS	GS_b^{Min}, GS_b^{Max}	300 Kcf/3500 Kcf
	$GS_b^{ch,\max}, GS_b^{dis,\max}$	300 Kcf/300 Kcf
	$\eta_b^{GSS,ch}/\eta_b^{GSS,dis}$	0.9/0.9
	$GS_{b,s,t=0}/GS_{b,s,t=24}$	300 Kcf
EB	η_b^{EB}	1
	$P_b^{EB,\max}$	80 MW